

# Material transport in $(\text{Ti}_{0.3}\text{W}_{0.5}\text{Cr}_{0.2})\text{B}_2$ ceramics: simultaneous diffusion of ion implanted $^{49}\text{Ti}$ and $^{54}\text{Cr}$

H. Schmidt<sup>a,\*</sup>, G. Borchardt<sup>a</sup>, C. Schmalzried<sup>b</sup>, R. Telle<sup>b</sup>, H. Baumann<sup>c</sup>,  
S. Weber<sup>d</sup>, H. Scherrer<sup>d</sup>

<sup>a</sup>*Abt. Thermochemie und Mikrokinetik, FB Physik, Metallurgie und Werkstoffwissenschaften, TU Clausthal, Robert-Koch-Str. 42, D-38678 Clausthal-Zellerfeld, Germany*

<sup>b</sup>*Institut für Gesteinshüttenkunde, RWTH Aachen, Mauerstr. 5, 52064 Aachen, Germany*

<sup>c</sup>*Institut für Kernphysik, J. W. Goethe-Universität, August-Euler-Str. 6, D-60486 Frankfurt, Germany*

<sup>d</sup>*Laboratoire de Physique des Matériaux, Ecole des Mines de Nancy, Parc de Saurupt, F-54042 Nancy Cedex, France*

Received 15 March 2002; received in revised form 12 June 2002; accepted 22 June 2002

## Abstract

Self-diffusion studies of Ti and Cr were carried out in a two-phase ceramic compound with nominal composition  $(\text{Ti}_{0.3}\text{W}_{0.5}\text{Cr}_{0.2})\text{B}_2$ , which is a model system for the development of in situ reinforced boride ceramics, via precipitation of a super-saturated host matrix. In the temperature interval  $1000\text{ }^\circ\text{C} \leq T \leq 1400\text{ }^\circ\text{C}$ , the diffusivities were determined with secondary ion mass spectrometry (SIMS) using co-implanted and simultaneously diffusing stable  $^{49}\text{Ti}$  and  $^{54}\text{Cr}$  isotopes. This procedure minimizes systematic errors, reduces experimental time, and enables a direct comparison of the results. The two-phase nature of the material is directly reflected in non-uniform Cr depth profiles, while for Ti, uniform depth profiles indicate nearly the same diffusivities in both phases. The diffusivities of both elements obey an Arrhenius behaviour with activation enthalpies of  $\Delta H^{\text{Ti}} = 3.1\text{ eV}$  and  $\Delta H^{\text{Cr}} = 3.3\text{ eV}$ , respectively, and very low pre-exponential factors of about  $D_0^{\text{Ti}} = 1 \times 10^{-9}\text{ m}^2/\text{s}$  and  $D_0^{\text{Cr}} = 6 \times 10^{-8}\text{ m}^2/\text{s}$ , which is a hint that no simple vacancy mechanism is operating in the material. The experimental results also suggest that the growth of the precipitates at  $1600\text{ }^\circ\text{C}$  is controlled by the volume diffusion of Cr and Ti.

© 2002 Elsevier Science Ltd. All rights reserved.

**Keywords:** Borides; Diffusion; Secondary ion mass spectrometry;  $(\text{Ti,W,Cr})\text{B}_2$

## 1. Introduction

A variety of phases of the quasiternary system  $\text{TiB}_2\text{--W}_2\text{B}_2\text{--CrB}_2$  are distinguished by large temperature dependent homogeneity ranges which are bordered by immiscibility gaps.<sup>1,2</sup> This peculiarity enables the tailored de-mixing of a supersaturated host matrix, leading to the formation of tungsten rich precipitates embedded in a  $(\text{TiWCr})\text{B}_2$  matrix. Under certain conditions, the precipitates may form elongated particles with a high aspect ratio.<sup>1</sup> These particles are well suited to improve the toughness and the creep resistance of the ceramic by in situ reinforcement of ceramic hard materials.<sup>1,3</sup>

For the production of reinforced ceramics it is of importance to understand and to quantitatively describe

the diffusion controlled changes in the microstructure occurring during precipitation and grain growth. The knowledge of the material transport mechanisms offers new ways to optimise microstructures and, consequently materials properties. Up to now, almost nothing is known on the atomic transport properties of these materials.

Quantitative investigations of atomic transport properties are commonly carried out by measuring the tracer diffusivities of the constituent elements. Because of the relatively low diffusivities in these materials, high spatial resolution in depth profiling is necessary. Thus, the diffusion measurements were performed with ion implanted stable isotopes as tracers and secondary ion mass spectrometry (SIMS). To obtain the temperature dependent diffusivities for all the elements which might contribute to the kinetic behaviour of the system, a large number of single diffusion experiments would be necessary. Therefore, we chose to co-implant and

\* Corresponding author. Tel.: +49-5253-72-2094; fax: +49-5253-72-3184.

E-mail address: harald.schmidt@tu-clausthal.de (H. Schmidt).

simultaneously diffuse the respective isotopes in order to determine diffusivities in the same sample in one experiment only and in one SIMS analysis, as well. This method has the advantage that the experimental errors are minimized, that the experimental time is significantly reduced, and that a direct comparison of the results is possible.

As a starting point for first investigations, a ceramic material with nominal composition  $(\text{Ti}_{0.3}\text{W}_{0.5}\text{Cr}_{0.2})\text{B}_2$  was used, showing good conditions for the growth of reinforcing platelets,<sup>4</sup> as only two phases are present, making the system under investigation not too complex.

## 2. Experimental procedure

The samples were produced by reaction sintering of high-energy milled powders of  $\text{TiB}_2$ , “WB<sub>2</sub>”, and  $\text{CrB}_2$  (H. C. STARCK, Germany) containing less than 1 wt.% of impurities. The reaction sintering process was carried out in a uniaxial hot press (die material: graphite) under a pressure of 60 MPa at 1800 °C for 30 min under argon atmosphere. Afterwards, the specimens were homogenized at 2000 °C for 8 h at ambient pressure and subsequently annealed for 6 h at 1600 °C in order to obtain de-mixing and precipitation. The samples were further examined by X-ray diffraction (XRD), secondary electron microscopy (SEM) and electron beam micro analysis (EPMA/EDX) in order to characterize phase content and microstructure.

For the diffusion measurements small platelets (about  $8 \times 8 \times 2 \text{ mm}^3$ ) were cut from the interior of the hot pressed samples, polished with diamond paste and cleaned with ethanol. The so prepared samples were implanted with a mass separated and scanned  $^{54}\text{Cr}^+$ -ion beam of 50 keV with a dose of  $5 \times 10^{15}$  ions/cm<sup>2</sup> at room temperature and afterwards with a  $^{49}\text{Ti}^+$ -ion beam at the same energy with a dose of  $1 \times 10^{16}$  ions/cm<sup>2</sup>. After tracer deposition, the implanted samples were diffusion annealed in the temperature range between 1000 and 1400 °C in argon atmosphere (1 bar) for times between 1 and 5 h. Tracer depth profiles (implantation and diffusion profiles) were measured by secondary ion mass spectrometry (VG SIMS-Lab), using a scanned  $\text{O}_2^+$ -ion primary beam (7 keV, 200 nA), detecting simultaneously  $^{49}\text{Ti}^+$  and  $^{54}\text{Cr}^+$  ions with a quadrupole mass spectrometer. Depth calibration was obtained by measuring the crater depth with a surface profilometer (Alphastep 500, TENCOR), assuming a constant sputter rate.

## 3. Results and discussion

XRD, REM and EDX measurements revealed that the samples with nominal composition  $(\text{Ti}_{0.3}\text{W}_{0.5}\text{Cr}_{0.2})\text{B}_2$  are

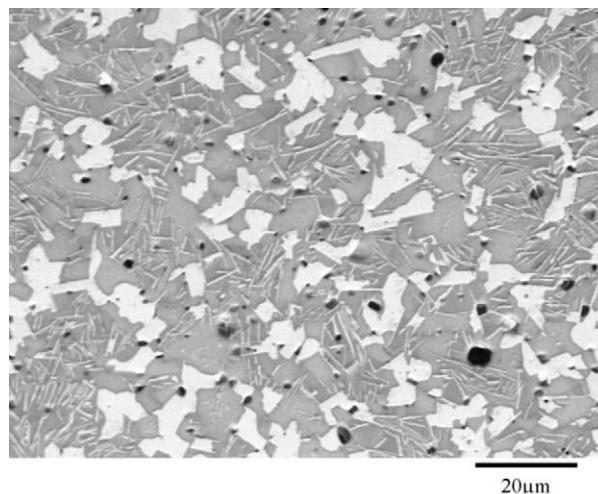


Fig. 1. SEM image of a two phase ceramic with nominal composition  $(\text{Ti}_{0.3}\text{W}_{0.5}\text{Cr}_{0.2})\text{B}_2$ , showing the solid solution matrix with an averaged composition of  $(\text{Ti}_{0.4}\text{W}_{0.3}\text{Cr}_{0.3})\text{B}_2$  (grey) and the platelet-like precipitates with a composition of  $(\text{Ti}_{0.03}\text{W}_{0.92}\text{Cr}_{0.05})\text{B}_2$  (white). The black regions are pores.

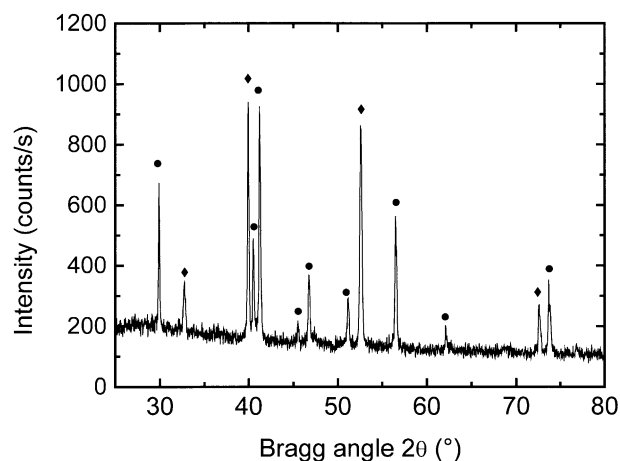


Fig. 2. X-ray diffractogram (CoK<sub>α</sub> radiation) of a  $(\text{Ti}_{0.3}\text{W}_{0.5}\text{Cr}_{0.2})\text{B}_2$  ceramic. The identified phases are: the matrix phase with  $\text{TiB}_2$  structure (diamond) and the precipitation phase with  $\text{W}_2\text{B}_5$  structure (circle).

separated into two phases (see Figs. 1 and 2). The matrix phase has  $\text{TiB}_2$  structure (space group:  $P6_3/mmm$ ) forming Ti, Cr, W solid solutions with approximate composition  $(\text{Ti}_{0.4}\text{W}_{0.3}\text{Cr}_{0.3})\text{B}_2$ . The second phase is a W-rich precipitation phase with  $\text{W}_2\text{B}_5$  structure (space group:  $P6_3/mmc$ ) showing a platelet-like habitus with a diameter of 5–10 μm and a thickness of only 0.5 μm. The precipitation phase exhibits a composition of  $(\text{Ti}_{0.03}\text{W}_{0.92}\text{Cr}_{0.05})\text{B}_2$  with a phase content of about 20–30%.

In Figs. 3 and 4 typical depth profiles of  $^{49}\text{Ti}$  and of  $^{54}\text{Cr}$  in  $(\text{Ti}_{0.3}\text{W}_{0.5}\text{Cr}_{0.2})\text{B}_2$  are displayed before and after annealing for various times and temperatures. The diffusion profiles of  $^{49}\text{Ti}$  show a uniform broadening of the nearly Gaussian implantation profile. The diffusivities  $D$  are obtained from the diffusion profiles by least-square

fitting the data to the following solution of Fick's second law<sup>5</sup>:

$$c(x, t) = \frac{A}{\sqrt{2\pi(\Delta R_p^2 + 2Dt)}} \exp\left(-\frac{(x - R_p)^2}{2\Delta R_p^2 + 4Dt}\right),$$

where  $c$  is the tracer concentration,  $t$  the diffusion time,  $A$  the implanted dose,  $R_p$  the projected range and  $\Delta R_p$  the standard deviation of the implantation profile.

On the contrary, the  $^{54}\text{Cr}$  depth profiles show two regions with different profile broadening (see Fig. 4). For the determination of the diffusivities the  $^{54}\text{Cr}$  profiles were fitted in each region separately by a Gaussian profile. In region A, no broadening of the diffusion profiles is measurable with increasing temperature within errors. A nearly constant value of about  $20 \pm 4$  nm is obtained for all annealed samples. In region B, however, appreciable profile broadening occurs as a function of temperature.

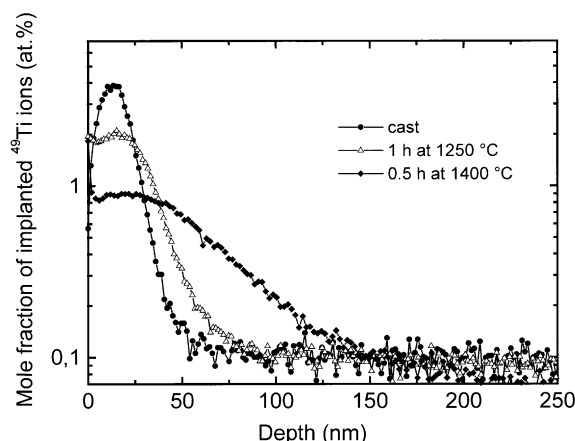


Fig. 3.  $^{49}\text{Ti}$  isotope depth profiles for ion-implanted polycrystalline  $(\text{Ti}_{0.3}\text{W}_{0.5}\text{Cr}_{0.2})\text{B}_2$  ceramics before and after annealing at different temperatures. For the sake of clarity, the natural background is subtracted.

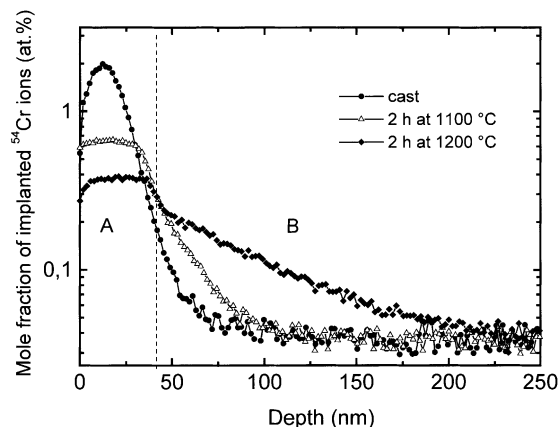


Fig. 4.  $^{54}\text{Cr}$  isotope depth profiles for ion-implanted polycrystalline  $(\text{Ti}_{0.3}\text{W}_{0.5}\text{Cr}_{0.2})\text{B}_2$  ceramics before and after annealing at different temperatures. For the sake of clarity, the natural background is subtracted.

Since the microstructural analysis revealed that the sample with nominal composition  $(\text{Ti}_{0.3}\text{W}_{0.5}\text{Cr}_{0.2})\text{B}_2$  is separated in the two crystallographic phases with composition  $(\text{Ti}_{0.4}\text{W}_{0.3}\text{Cr}_{0.3})\text{B}_2$  and  $(\text{Ti}_{0.03}\text{W}_{0.92}\text{Cr}_{0.05})\text{B}_2$ , which might have different diffusivities, the obtained isotope depth profiles have to be interpreted in that context. For the case of Ti diffusion, the observed uniform depth profiles indicate a comparable size of the diffusivities in both phases. This leads to an effective diffusivity of the two-phase material describing the overall diffusion behaviour. In contrast, the two regions A and B observed for the Cr depth profiles can be explained with the assumption that the two crystallographic phases have different diffusivities at a given temperature. Region B reflects the diffusion in the phase with the higher diffusivity which is responsible for the long range atomic transport in the material. Region A represents the other phase whose diffusivities are considerably lower, at least smaller than  $1 \times 10^{-20} \text{ m}^2/\text{s}$  at  $1100^\circ\text{C}$ . A further analysis of region A is not possible due to insufficient profile broadening and overlapping with the profile of region B. From numerical integration of the fitting profiles in each region we can approximately determine the amount of diffused tracer present in each phase. A ratio of about 3:1 is obtained within errors, which corresponds well to the phase content of both phases in the sample (70–80% matrix phase and 20–30% precipitation phase), as determined by X-ray diffractometry. From these findings we assume that the phase with the lower diffusivities is the precipitation phase  $(\text{Ti}_{0.03}\text{W}_{0.92}\text{Cr}_{0.05})\text{B}_2$  and that with the larger diffusivities is the matrix phase  $(\text{Ti}_{0.4}\text{W}_{0.3}\text{Cr}_{0.3})\text{B}_2$ . For a better understanding, the diffusion process in the two-phase material is illustrated schematically in Fig. 5.

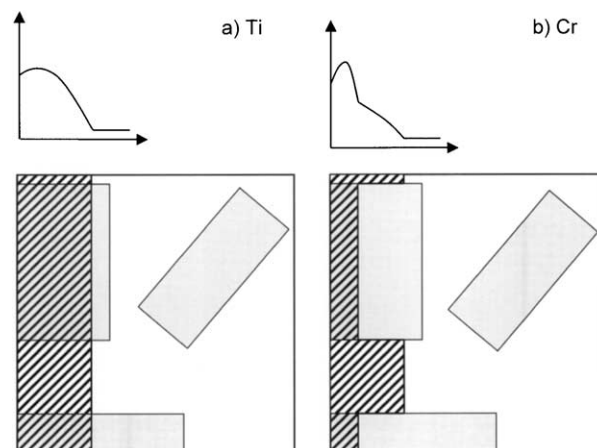


Fig. 5. Schematic illustration of the diffusion process in the two-phase ceramic  $(\text{Ti}_{0.3}\text{W}_{0.5}\text{Cr}_{0.2})\text{B}_2$  for the tracers a) Ti and b) Cr. The matrix phase  $(\text{Ti}_{0.4}\text{W}_{0.3}\text{Cr}_{0.3})\text{B}_2$  is displayed in white, the precipitation phase  $(\text{Ti}_{0.03}\text{W}_{0.92}\text{Cr}_{0.05})\text{B}_2$  in grey and the penetration of the diffusion front is hatched. The isotope depth profiles are also sketched for illustration.

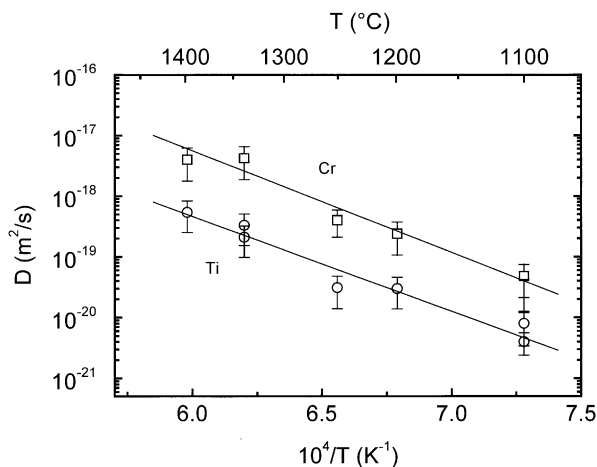


Fig. 6. Diffusivities of  $^{49}\text{Ti}$  and  $^{54}\text{Cr}$  in polycrystalline  $(\text{Ti}_{0.3}\text{W}_{0.5}\text{Cr}_{0.2})\text{B}_2$  as a function of reciprocal temperature.

Fig. 6 shows the self-diffusivities of  $^{49}\text{Ti}$  and  $^{54}\text{Cr}$  in  $(\text{Ti}_{0.3}\text{W}_{0.5}\text{Cr}_{0.2})\text{B}_2$  as a function of reciprocal temperature as obtained from the depth profiles of Ti and from the depth profiles of Cr in region B. The diffusivities for both elements can be described by an Arrhenius relation within the temperature range from 1100 °C to 1400 °C according to

$$\left[ D = D_0 \exp\left(-\frac{\Delta H}{kT}\right) \right]$$

where  $D_0$  denotes the pre-exponential factor,  $\Delta H$  the activation enthalpy and  $k$  the Boltzmann constant. The activation enthalpies are determined as  $\Delta H^{\text{Ti}} = 3.1 \pm 0.5$  eV and  $\Delta H^{\text{Cr}} = 3.3 \pm 0.5$  eV, respectively, and the pre-exponential factors are  $D_0^{\text{Ti}} = 1.1 \times 10^{-9}$  m<sup>2</sup>/s and  $D_0^{\text{Cr}} = 6.4 \times 10^{-8}$  m<sup>2</sup>/s. The Ti diffusivities are about 1 order of magnitude smaller than those of Cr in the whole temperature range investigated.

The diffusion of both elements is relatively slow considering the melting temperature  $T_m$  of the ceramic material of about 2000–2100 °C.<sup>1</sup> An extrapolation of the data to  $T_m$  yields diffusivities of about  $10^{-15}$ – $10^{-16}$  m<sup>2</sup>/s, which is more typical for semiconductors than for metals<sup>6</sup> and reflects the influence of covalent bonding in these materials. For the empirical ratio  $\Delta H/T_m$  we obtain values of  $1.4 \times 10^{-3}$  eV/K which is, however, in fair agreement with typical values of  $1.5 \times 10^{-3}$  eV/K obtained for metals.<sup>6</sup> This shows that the activation enthalpy is not anomalously low in these materials. In contrast, the pre-exponential factors  $D_0$  in the order of  $10^{-9}$ – $10^{-8}$  m<sup>2</sup>/s are extremely low as compared with those commonly found for self-diffusion in metals (typically  $10^{-4}$ – $10^{-6}$  m<sup>2</sup>/s).<sup>6</sup> Using the relation  $D_0 = f a^2 \nu_0 \exp(\Delta S/k)$ , where  $f \approx 1$  is the correlation factor,  $a \approx 0.3$  nm the jump distance,

and  $\nu_0 \approx 10^{13}$  1/s the effective attempt frequency, the entropy of diffusion  $\Delta S$  can be calculated. Hence a negative entropy of diffusion of  $\Delta S = -6.8$  k for Ti and of  $\Delta S = -2.8$  k for Cr is derived, which is the reason for the small diffusivities. This might be a hint that no simple vacancy mechanism is operating in the material.

The diffusion lengths  $d = 2\sqrt{Dt}$  at 1600 °C, the temperature where the de-mixing of the ceramic was carried out, are determined by linear extrapolation of the measured diffusivities to about  $d^{\text{Ti}} = 0.8$  μm and  $d^{\text{Cr}} = 2$  μm, respectively, for an annealing time of 6 h. This is in the same order of magnitude as the radius of the precipitates of about 2–5 μm and the average distance between the precipitates of about 5 μm (see Fig. 1). Assuming a diffusion controlled growth of the precipitates, the volume diffusivities of Cr and Ti might be the determining kinetic parameter for the formation of the platelets.

#### 4. Conclusion

From self-diffusion studies of the elements Ti and Cr in a two-phase ceramic of nominal composition  $(\text{Ti}_{0.3}\text{W}_{0.5}\text{Cr}_{0.2})\text{B}_2$  the following conclusions can be drawn: the tracer depth profiles for the Cr isotope showed that the presence of two crystallographic phases is reflected directly in the diffusion behaviour. The observed non-uniform depth profiles indicate that the Cr diffusivities in the two phases are different by at least a factor of 10. A quantitative analysis was possible only for the fast diffusing phase, which is identified as the matrix phase  $(\text{Ti}_{0.4}\text{W}_{0.3}\text{Cr}_{0.3})\text{B}_2$ . In contrast, for Ti the diffusivities of both phases are of comparable volume, leading to uniformly distributed isotope profiles and an effective mean diffusion coefficient. The obtained diffusivities obey an Arrhenius behaviour with activation enthalpies of  $\Delta H^{\text{Ti}} = 3.1$  eV and  $\Delta H^{\text{Cr}} = 3.3$  eV and very low pre-exponential factors of about  $D_0^{\text{Ti}} = 1 \times 10^{-9}$  m<sup>2</sup>/s and  $D_0^{\text{Cr}} = 6 \times 10^{-8}$  m<sup>2</sup>/s, corresponding to a negative entropy of diffusion. This might be a hint that no simple vacancy mechanism is operating in the material. The experimental results are in agreement with a model which describes the formation of the precipitates at 1600 °C as a growth process controlled by the diffusivities of Cr and Ti.

#### Acknowledgements

The authors would like to thank E. Ebeling for ceramographic preparation of the samples and for technical support and A. Mühlhan for her assistance in SEM analysis. This work has been funded by the Volkswagenstiftung.

## References

1. Mitra, I. and Telle, R., Phase formation during anneal of supersaturated  $\text{TiB}_2\text{--CrB}_2\text{--WB}_2$  solid solutions. *J. Sol. State Chem.*, 1997, **133**, 25.
2. Telle, R., Fendler, E. and Petzow, E., The Quasi-binary Systems  $\text{CrB}_2\text{--TiB}_2$ ,  $\text{CrB}_2\text{--WB}_2$ , and  $\text{TiB}_2\text{--WB}_2$ . *J. Hard Mater.*, 1992, **3**, 211.
3. Schmalzried, C., Telle, R., Freitag, B. and Mader, W., Solid state reactions in transition metal diboride based materials. *Z. Metallkd.* **92**, (2001), 1197, and references cited therein.
4. Mitra, I., Gefügeentwicklung und Plättchenwachstum im System der Übergangsmetallboride  $\text{TiB}_2$ ,  $\text{W}_2\text{B}_5$  und  $\text{CrB}_2$  zur Dispersionsverstärkung von Carbidkeramik. PhD thesis, RWTH Aachen, 1998.
5. Ryssel, H. and Runge, I., *Ion Implantation*. Wiley and Sons, Chichester, 1986 95.
6. Philibert, J., *Atom Movements*. Les Editions de Physique, Les Ulis, 1991 122 ff.